



OPEN Perception and communication of relevant colours in paintings by observers with colour vision deficiencies

Juan Luis Nieves✉, Javier Hernández-Andrés, Luis Gómez-Robledo & Javier Romero

In a previous work, we empirically analysed the so-called “relevant colours” in paintings. These relevant colours describe the number of colours that stand out for an observer when glancing at a painting. On average, 19 relevant colours were identified, enabling reliable segmentation of colour images via a small palette of colours. The purpose of this study was to analyse how observers with different colour deficiencies (specifically, 11 deuteranopes, 11 protanopes, 3 deuteranomalous and 4 protanomalous observers) perceive the most representative colours in paintings. To achieve this, a set of painting images was presented to these observers. They were instructed to mark those areas within the image that contained a relevant colour via a mouse. The observers visually scanned the entire painting and selected pixels belonging to relevant chromatic areas. The study included 20 images from the Prado Museum in Madrid, Spain. The results revealed that, as expected, the average number of relevant colours identified by all observers was relatively small, consisting of only 9 colours. This number was lower than the average number of colours found for observers with normal colour vision in the earlier study and reveals that dichromatic observers experience a degradation in their mental impressions of the observed paintings. Nevertheless, the results indicate that there is almost no difference in the number of relevant colours obtained between the two types of colour vision deficiencies; deuteranopes seem to be able to use more relevant colours than protanopes need for the same painting (10 and 8 relevant colours, respectively). By analysing the segmentation of pictorial scenes with relevant colours identified for each painting as colour seeds, we inferred how colour-deficient observers perceive and communicate much of the critical chromatic content in a painting. Through maximizing communicative effectiveness and minimizing the cognitive load, our results assess the colour information retained by anomalous observers, indicating that they lose approximately 20% of the representational content compared with normal observers.

Visual perception involves the interpretation of visual cues and information and is usually described in terms of three main processes, encoding, selection, and decoding, which ultimately lead to a motor action and/or a cognitive decision, such as a perceptual response^{1,2}. Differences in these processes underlie the impairment in chromatic diversity developed by dichromats and, of course, in the colour discrimination capabilities of the observers with colour vision deficiencies^{3–6}. However, the colour perception of dichromats when they are observing complex images such as paintings, either for their spatial or chromatic complexity, has not yet been extensively analysed. Recent studies⁷ have begun to explore the colour perception of dichromats when observing complex images like paintings. Compared with normal observers, perceived gamut differs, but what is the colour perception of a painting from the perspective of the dichromats themselves? Therefore, how is colour perception of paintings affected by inherited colour vision deficiencies? Within the restricted colour gamut perceived by defective observers, are dichromatic observers able to extract the relevant colours that describe paintings (i.e., their mental representations)?

In a seminal paper from 2010, it was found that the average number of perceptually distinct surface colours was estimated as much smaller than that based on counting methods⁸. Nevertheless either the process of how relevant colours (those that are more representative or attract more attention in an image) are selected by observers nor how they are coded and decoded in the visual cortex is currently well understood. In previous works^{9,10}, we introduced the concept of “relevant colours” of an image, which allowed us to estimate the number of colours that an observer would perceive as prominent in a glance at the image. These relevant colours

Department of Optics, University of Granada, 18071 Granada, Spain. ✉email: jnieves@ugr.es

enable us to evaluate not only the discernible colours that are chromatically distinct in the scene but also the colour palette of the image. The relevant colour concept was psychophysically confirmed recently¹¹, and it was demonstrated that those colours are consciously used by observers with normal colour vision when they visualize the spatio-chromatic content of colour images. In addition, each original image can be segmented based on its corresponding relevant colour set, which describes the colour palette of the painting and leads to efficient quantization¹².

Colour vision deficiencies, including dichromacy and anomalous trichromacy, have been extensively investigated in the field of vision science. The reviewed studies encompass various aspects, such as the impact of natural scene colour distributions on perceived chromatic diversity^{10,12}, estimation of discernible colours for colour-deficient observers^{4,13}, the role of coloured lenses in colour discrimination^{14–16}, the use of complex scenes and Munsell samples in predicting chromatic changes, spatial visual function in anomalous trichromats, and saliency-based image correction for observers with colour vision deficiencies. Investigating the impairment of colour discrimination in dichromacy, Linhares et al.¹⁷ revealed that estimates based solely on the number of discernible colours do not fully capture the perceived chromatic diversity in natural scenes. By considering the actual distributions of colours, dichromats can discriminate a greater percentage of colour pairs than anticipated, highlighting the beneficial influence of colour distributions in natural scenes. Perales et al.⁴ estimated the number of colours perceived by individuals with colour vision deficiencies via models that simulate the appearance of stimuli. The findings demonstrate a significant reduction in the number of discernible colours for dichromats. Anomalous trichromats, on the other hand, retain some of the colour discriminability that is lost in dichromats, with the level of impairment varying depending on the specific anomaly.

Other authors^{18–20} have also shown that dichromats can use different basic colour terms and have a different pattern of colour preference than do trichromats, with a preference for yellow and a weaker preference for blue. The preferences were more affected in individuals who lacked the cone type sensitive to long wavelengths (protanopes) than in those who lacked the cone type sensitive to medium wavelengths (deuteranopes). The relationship between colour preference and colour naming revealed that colours that are easier to name are preferred by those observers with colour vision deficiencies, providing insight into how dichromats would experience aesthetics. In addition, inherited red–green colour vision deficiency affects approximately one in twelve men of European descent, impacting tasks such as foraging, detecting blushing, or breaking camouflage. However, its effect on real-world vision is less clear. The results from Foster and Nascimento²¹ have shown that individuals with red–green deficiency lose only a small amount of information compared with those with normal colour vision, with factors such as large lightness variations, small redness–greenness differences, and uneven surface colours helping to minimize the impact.

The objective of this study is to obtain a comprehensive dataset of relevant colours observed in different colour images with varied spatio-chromatic content on the basis of the experiences of individuals with colour vision deficiencies. Determining and analysing these relevant colours will allow us to compare the perception of colour palettes among colour-deficient observers and those with normal colour vision. In addition, potential applications in image compression can be exposed after the amount of information retained by anomalous colour observers is estimated.

Compared with individuals with normal colour vision, colour-deficient observers clearly have a restricted range of perceived colours. However, the extent of chromatic information they are missing remains uncertain²², as they do not have the original image with all its colours to be aware of the potential loss of information (unless the deficiency occurred at a specific point in their lives). The previous work by Tirandaz et al.¹² demonstrated that observers with normal colour vision are efficient at quantizing coloured images by reducing the number of colours in paintings to a small subset they deem relevant. Estimating the mutual information between each original image and its quantized representation based on relevant colours was sufficient for that purpose. Nevertheless, in the current work, the results will be influenced in two ways: first, by the amount of information or resources required to encode the signal (due to the use of the relevant colours paradigm), and second, by the loss of fidelity introduced during reconstruction (as the experiment is conducted with observers who have anomalous colour vision). The rate-perception distortion theory^{23,24} will be used to untangle that interconnection. We will assume that the set of all colours from a simulated colour vision deficiency (CVD) image is the “true” probability function and that the set of relevant colours obtained from anomalous observers is the “perceived” probability function. How “relevant” are the colours selected by colour-deficient individuals compared to the relevant colours chosen by individuals with normal colour vision? Does the palette of relevant colours from individuals with normal colour vision align with that of anomalous observers for the same image? This study aims to explore the visual similarity between colour palettes and the information shared by both sets of colours.

Figure 1 shows the set of test images used in the experiment. The images were selected because of their intricate spatio-chromatic content and realistic nature. They represent a subset of previously used representational paintings, for which observers with normal colour vision estimate their relevant colours⁹.

Results

Number of relevant colours

Figure 2 shows the number of relevant colours (NRC) found for all observers and paintings. The global NRC average found in the experiment was 9 ± 2 colours. This is a 53% reduction in comparison with the 19 ± 5 previously reported for normal observers¹¹. Interestingly, the expected reduction in the number of colours found was accompanied by a similarly low standard deviation in comparison to normal colour vision.

The comparison between different CVDs is shown in Fig. 3, where the number of relevant colours is plotted separately for the deuteranope and protanope observers and the deuteranomalous and protanomalous observers. For protanopes, the NRC is slightly lower but does not appear to be significant compared with the average.



Fig. 1. Montage of images of conventionally representational paintings in the Prado Museum²⁸, adapted from Nieves et al.¹⁰, Fig. 1, licenced under CC BY 4.0 (the colour gamuts of each of these images are illustrated in Fig. 4 from Tirandaz et al.¹²).

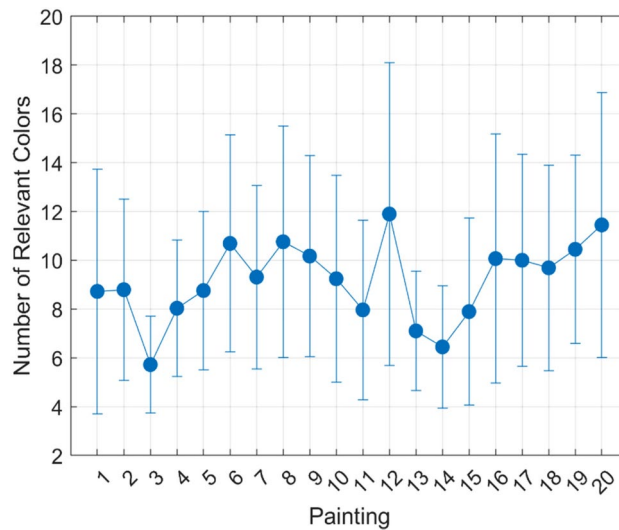


Fig. 2. Number of relevant colours. Estimated average of the number of relevant colours for all observers and paintings used in the study (error bars represent 1 SD).

Deuteranopes obtained a slightly higher NRC (although not on average) due to paintings 5, 8, and 12. These differences are reduced among deuteranomalous and protanomalous observers.

Efficient representation of colour images by relevant colours

Figure 4 shows the estimated mutual information between each image in Fig. 1 and its quantized representation by relevant colours. The data are for each of the 20 paintings averaged for all individual observers; the boxplot

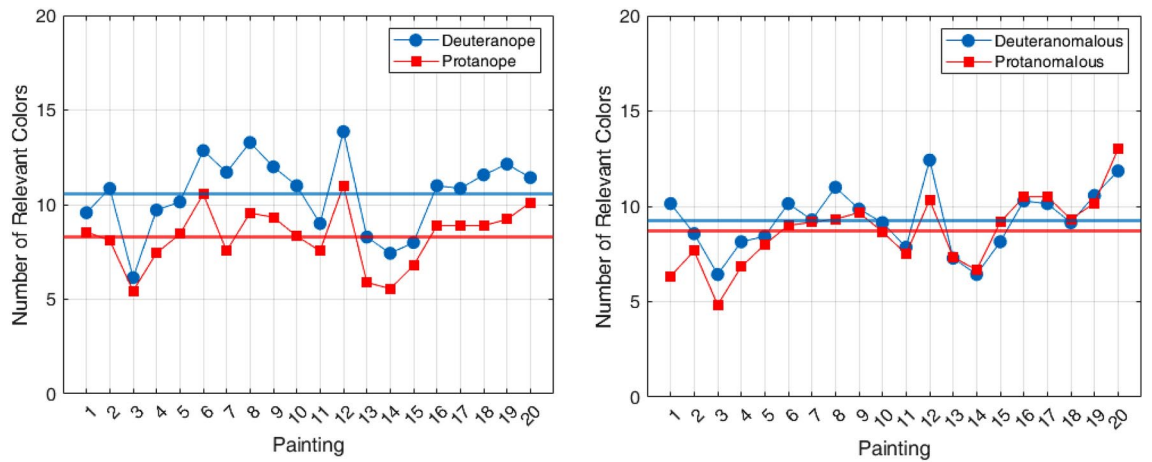


Fig. 3. Number of relevant colours from colour anomalies. Estimated number of relevant colours for (left) Deuteranopes and Protanopes observers and (right) Deuteranomalous and Protanomalous observers. The horizontal lines represent the average number of relevant colours for each kind of anomaly.

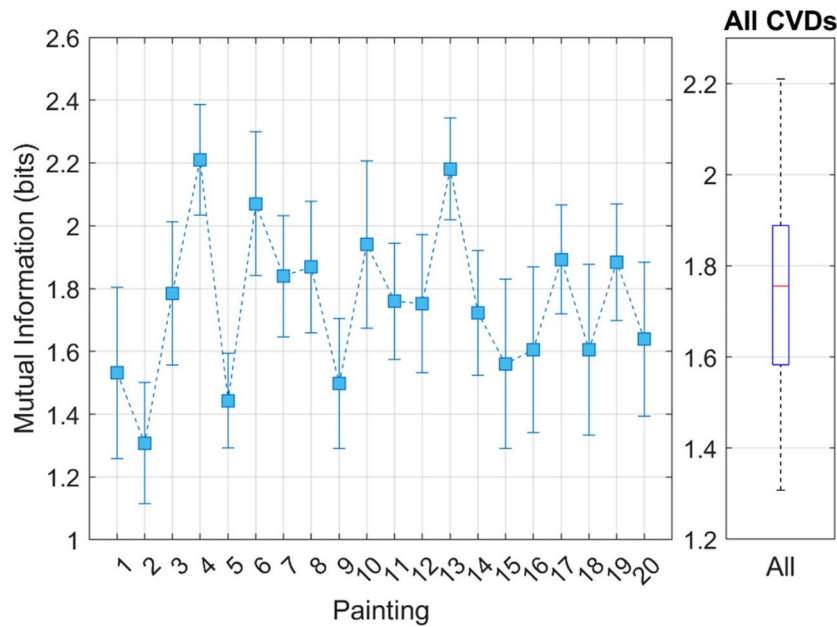


Fig. 4. Information from relevant colours. Mutual information for each painting averaged across observers. The right plot shows the global average mutual information for all observers and paintings (the central mark indicates the median, and the lower and upper edges of the box represent the 25th and 75th percentiles, respectively; the whiskers extend to the most extreme data points that are not considered outliers).

on the right summarizes the global results for all observers and paintings. The mutual information values varied between a minimum of 1.3 bits (for painting number 2) and a maximum of 2.2 bits (for paintings number 4 and 13). Apart from those differences, all estimated mutual information values were similar, and a global average of approximately 1.75 bits was obtained. The value of mutual information obtained for colour-deficient observers is thus lower than that obtained from approximately 2.2 bits for normal observers (see Fig. 2 on Tirandaz et al.¹⁰). This means that, on average, colour-deficient observers lose 26% of the representation by relevant colours used by normal observers for the same image dataset.

Figure 5, which analyses MI values per anomaly, shows how the mutual information on average is slightly greater in deuteranopes (1.8 bits) than in protanopes (1.7 bits), whereas for anomalous trichromats, there is no difference in the mean values (1.7 bits for deuteranomalous and protanomalous).

The previous results show, as expected, that observers with colour vision deficiencies lose information during image observation. However, the percentage of loss does not seem very large, at least compared with the severity of the deficiency. To illustrate this loss of relevant information in some way, the images in Fig. 1 have been

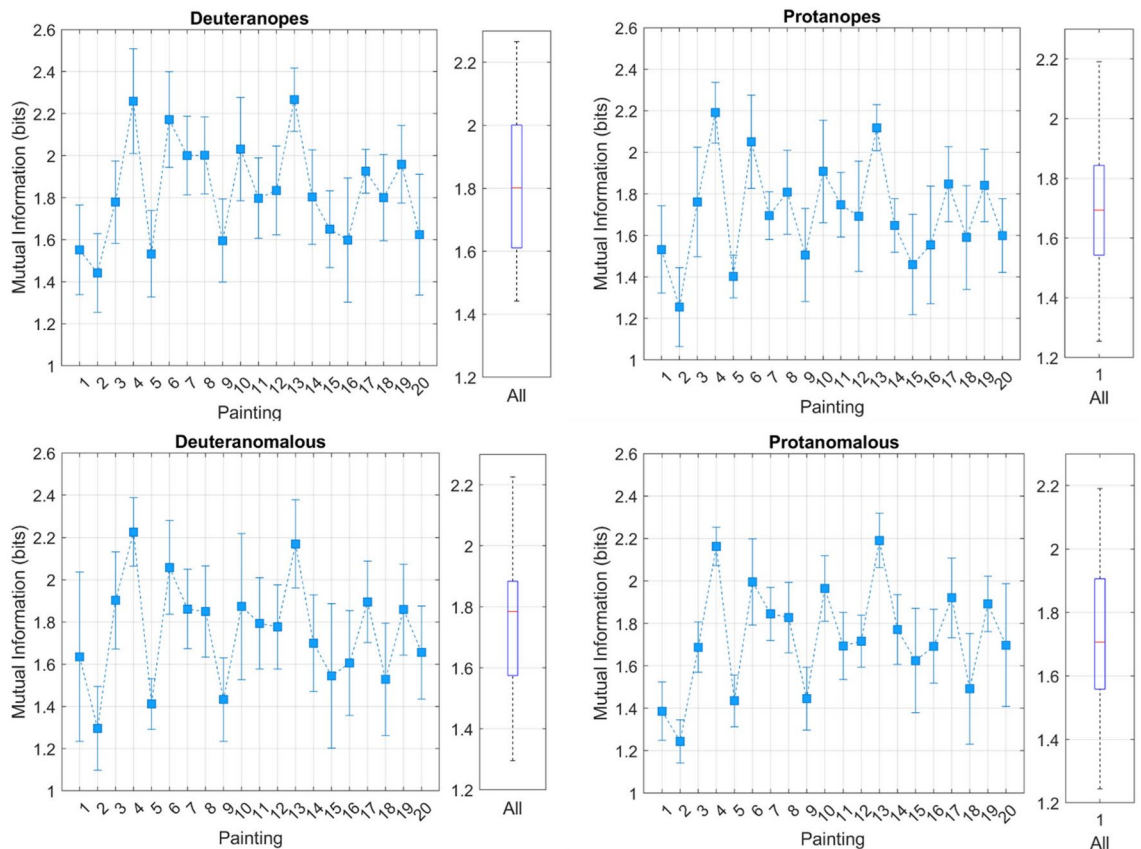


Fig. 5. Information from relevant colours and colour anomalies. Mutual information for each painting averaged across observers. The upper row corresponds to deuteranopes and protanopes, whereas the lower row corresponds to deuteranomalous and protanomalous observers. On the right-hand side of every plot, the global average mutual information for all observers and paintings is shown (the central mark indicates the median, and the lower and upper edges of the box represent the 25th and 75th percentiles, respectively; the whiskers extend to the most extreme data points that are not considered outliers).

segmented by relevant colours. That is, taking the relevant colours as seeds, it is possible to find the nearest pixels to a relevant colour for each image and assign that colour to them. Representing each image in this way provides an idea of the mental representation that each observer would have of the images^{10,11}.

Figure 6 shows examples of the distribution of original colours in a^*b^* and the selected relevant colours, as well as the original image number 8 (one of those with the greatest variety of colours). To provide valuable insights into the effectiveness of the segmentation process in preserving information and capturing colour diversity from the original images, we computed the normalized preservation of mutual information between original and experimentally segmented images¹². The approximately uniform colour space CIELAB was divided into cubic cells whose side length was a multiple of the smallest discriminable step, and colorimetric arguments were then used to assign the colours of a scene to those cells. From each set of observer-selected relevant colours, a colour palette was extracted and applied to the painting by assigning relevant colours to areas occupied by pixels close to those colours. A look-up table was built for each image, calculating the distance between every pixel in the original image and the colours in the table. The closest match determined the new relevant pixel colour¹⁰.

The results in Fig. 7 show that, first, the representation of images by relevant colours effectively preserves most of the information, leading to a surprisingly good representation despite theoretical colorimetric considerations (as the previous figures above have shown), except for image number 7 and protanope observers, which preserved the MI to 60%. In contrast, images such as those 4 and 10 had high representational values of approximately 90%. Second, deuteranope observers obtained slightly better preserved MI values (approximately 82% on average) than did protanopes (75% on average). The differences for anomalous trichromats are even less relevant, with a preserved MI of approximately 78% on average for both kinds of anomalies.

Interplay of mutual information, redundancy, and rate-distortion theory in colour vision deficiencies

Now, within the above results, how efficient is an anomalous observer in processing space-colour information compared with a normal observer performing the same task? How does this efficiency vary on the basis of the complexity of the observed stimuli? Rate-distortion theory²⁴, a cornerstone of information theory, serves as a

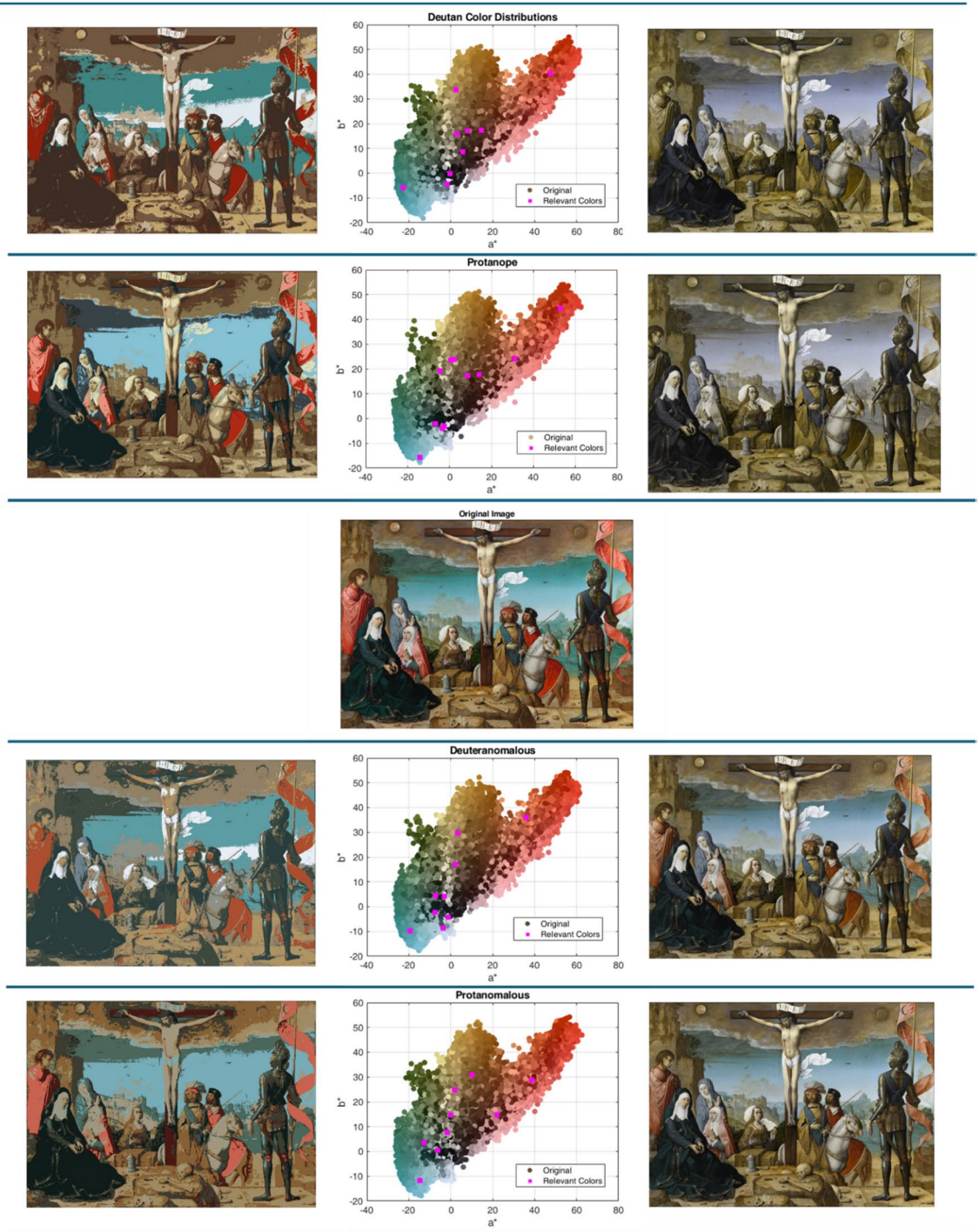


Fig. 6. Quantized segmentation of images by relevant colours. Image representations are for (left side) segmented images by relevant colours and (right side) simulated CVD images for painting no. 8 in Fig. 1. The first and second rows represent deuteranope and protanope observers, while the fourth and fifth rows represent deuteranomalous and protanomalous observers. In the central column, the distributions of colours in the CIE a^*b^* colour plane are shown with both the original colours and the relevant colours selected by some observers. CVD simulations were generated using the Machado et al. model³⁴ with $d = 20$ nm for deuteranope and protanope examples, and $d = 8$ nm for deuteranomalous and protanomalous examples. The original full colour image is also shown at the centre for comparison. (Images and plots were generated using MATLAB, R2023b, MathWorks, <https://www.mathworks.com/>).

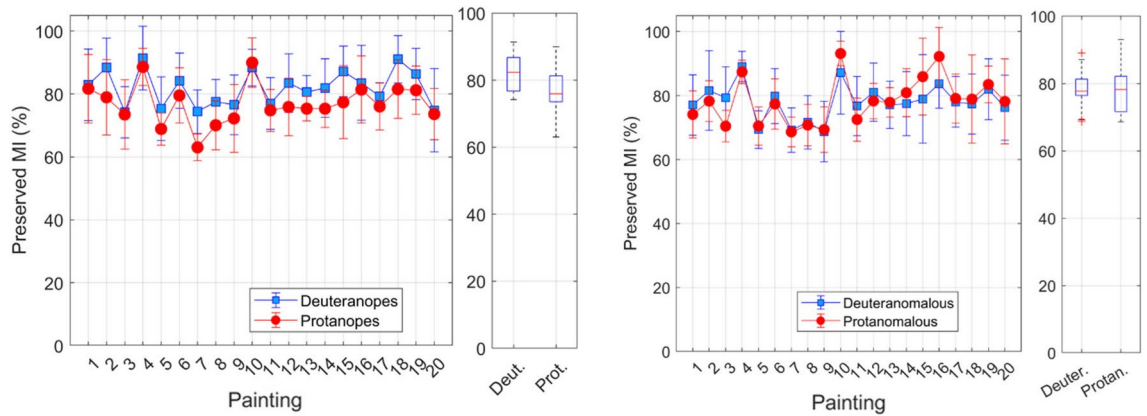


Fig. 7. Normalized preservation of mutual information between original and experimentally segmented images for (left) deuteranopes and protanopes and (right) deuteranomalous and protanomalous observers. The box plots close to each panel represent the global averages for the corresponding observers and paintings (the central mark indicates the median, and the lower and upper edges of the box represent the 25th and 75th percentiles, respectively; the whiskers extend to the most extreme data points that are not considered outliers).

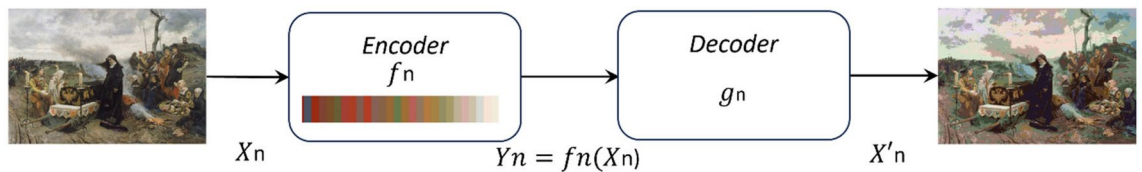


Fig. 8. A schematic overview of rate–distortion theory tailored to the relevant colour paradigm. An observer needs to refer to original colours X_n (associated with the original image on the left-hand side). To achieve this, the observer applies a probabilistic rule f_n to encode a sequence of colours X_n . The resulting encoded sequence of colours Y_n is fed to a decoder g_n , which produces a set of relevant colours X'_n in place of the actual colour X_n (represented here on the segmented image on the right-hand side of the figure). This process hinges on the perceptual distortion that arises from substituting X_n for X'_n . By selecting the relevant colour X'_n , the observer reduces the uncertainty in the communication of the true colour, an effect quantified, on average, by the accuracy and complexity linked to the process. (Images were generated using MATLAB R2023b, MathWorks, <https://www.mathworks.com/>), and text and graphical elements were added using GIMP 2.10.36, <https://www.gimp.org/>).

profound framework for understanding the interplay between complexity and accuracy in systems tasked with representing, processing, or transmitting information. At its core, rate-distortion theory explores the balance between the rate R —the amount of information or resources required to encode a signal—and the distortion D —the loss of fidelity introduced during reconstruction. This trade-off is encapsulated by the function $R(D)$, which delineates the minimum information rate needed to achieve a desired level of distortion D . As distortion decreases (or fidelity increases), the required rate inevitably grows, reflecting the rising complexity of representation. This principle mirrors the dynamics of complexity and accuracy measurements in signal processing, vision, and imaging.

In terms of the rate-distortion theory, let us consider a colour-deficient encoder, denoted as f_n , which encodes a sequence of colour X_n . As illustrated in Fig. 8, the resulting encoded sequence Y_n is then fed to a decoder, represented by g_n . The decoder outputs a sequence X'_n , which represents the most relevant colours in a scene. Thus, it is reasonable to address the following question: what is the best rate R to achieve for distortion at max D ? That is, if the target distortion of a colour-defective lossy compressor is D , what is the best method for compressing the data?

On the one hand, the resources—whether computational, informational, or biological—required to process or represent data are represented by the complexity $I_q(M; W)$, which is given by the information rate

$$I_q(M; W) = \sum_{M,W} p(m) q(M) \log \frac{q(M)}{q(W)} \tag{1}$$

where the observer represents the intended meaning M by W , using an encoder $q(M)$. If useful communication is preserved, W must contain some information about M (i.e., complexity must be greater than zero). In this case, complexity is computed as the mutual information between each original colour image and its corresponding

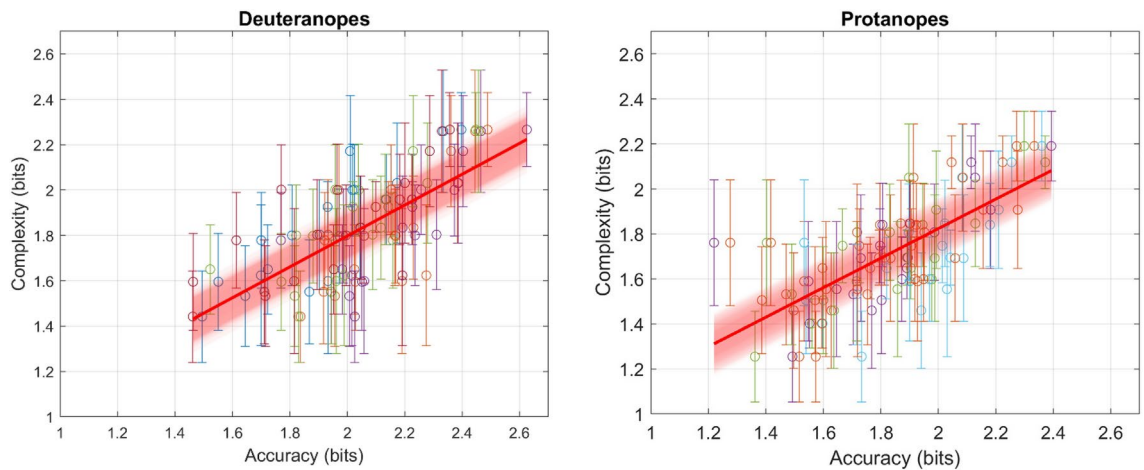


Fig. 9. Communication of relevant colours by (left) deuteranopes and (right) protanopes observers. Every point represents the accuracy (on the x-axis) versus complexity (on the y-axis) for all observers. A linear regression of the data is shown, with 95% confidence intervals highlighted in red, to better illustrate the general trends.

relevant colour image derived from CVD observers, which is essentially the same as mutual information in previously presented results.

On the other hand, how well a system performs a given task or reconstructs the original information is quantified through the accuracy, which is inversely related to the cost of misunderstanding or distorted meaning. Thus, the accuracy $I_q(W; U)$ is directly related to Shannon's mutual information $I(M; U)$ as

$$I_q(W; U) = I(M; U) - E_q \left[D \left(\hat{M} \right) \right] \quad (2)$$

where $E_q \left[D \left(\hat{M} \right) \right]$ is the Kullback–Leibler divergence, which is indicative of distortion. By minimizing distortion, we can maximize the accuracy (i.e., informativeness) quantified by $I_q(W; U)$. Accuracy is computed as the mutual information between each theoretical CVD image and each of its corresponding relevant colour images.

Figure 9 shows the results for the obtained information plane (i.e., accuracy versus complexity) for the communication of relevant colours by deuteranopes (left) and protanopes (right) observers. Accuracy in this context refers to how closely the segmented and compressed images (perceived by an ideal colour-deficient observer) match the original images in terms of perceptual quality. For a given complexity, high accuracy indicates that the segmented images closely resemble the theoretical segmentation, demonstrating effective preservation of perceptual details. Although, to the best of our knowledge, no established benchmarks for accuracy and complexity levels are directly applicable to our data, accuracy and complexity values within the range [1–2.5] have been found²⁵. Our results in Fig. 9 are around those values and suggest that deuteranope observers achieve slightly higher accuracy for higher complexity values. In contrast, protanope observers cover a wider range of low complexity values, reaching lower values (below 1.42, which is the minimum for deuteranopes). In the high complexity range, there do not seem to be differences between the two types of observers. The figures show the linear fits with a 95% confidence interval, indicating that the slopes are almost the same and less than one for both types of observers.

Discussion and conclusions

The visual system employs various mechanisms to encode colour information in a way that prioritizes the most informative aspects and reduces redundancy, ensuring efficient transmission of colour information to the brain. A person with normal colour vision already must pay a 'cost' in terms of lost information when observing a scene owing to the inherent structure of the human visual system (finite number of photoreceptors in the retina and a limited number of nerve cells at the optic nerve exit, creating a bottleneck). Nevertheless, the human visual system has proven to be efficient in perceiving complex images^{10,12}. It is logical to assume, therefore, that if this holds true for a normal observer, the cost for an anomalous observer undertaking the same perceptual task would be much greater. Limiting factors in the amount of information to process are now compounded by restrictions on the types of photoreceptors available, depending on the severity of the anomaly or the decrease in discriminative capacity for less severe anomalies.

We inferred how colour-deficient observers communicate the most relevant colours that appear in a painting. The distribution of relevant colours confirms, as expected, that observers with colour vision deficiencies miss colour information available to normal trichromatic observers when viewing a painting. Nevertheless, our analysis provides support for the notion that those deficient individuals retain the most relevant colour content of the observed painting, which aligns with the compression of information imposed by a particular CVD.

Compared with normal observers, these observers lose approximately an additional 20% in the representation of images by relevant colours. That 20% corresponds to about 0.5 bits which correspond to a reduction of about 30% in the number of distinguishable colours. Overall, our results are consistent with and almost exactly like those of Foster and Nascimento²¹, who reported that information is only slightly reduced in red–green colour vision deficient observers compared with normal trichromatic observers. Of course, those predictions were made for natural scenes, not paintings. But as demonstrated by Montagner and colleagues²², paintings and natural scenes share many statistical chromatic properties. Certainly, the MI range we found for protanopes and deuteranopes appears slightly lower (approximately 1.2–2.2 bits) than the MI values reported for clustering methods in the findings of Tirandaz et al.¹², which extend up to 3 bits. Interestingly, the number of relevant colours and the mutual information values did not differ substantially between dichromats and anomalous trichromats, which is somewhat surprising. This would suggest that despite their differences in the underlying colour perception mechanisms, the ability of these observers to encode chromatic information in a meaningful way remains strikingly similar. This finding may provide insights into compensatory processes or shared strategies employed by colour vision-deficient observers to interpret complex visual scenes. As noted by Zhaoping and Geisler²⁶, protanopes and deuteranopes are expected to have significantly higher thresholds in the long-wavelength region than trichromats. Their predictions suggest that, for trichromats, wavelength discrimination at short wavelengths is mediated by the protanopic/deutanopic system and that at long wavelengths, it is mediated by the tritanopic system (see Fig. 7 in Zhaoping and Geisler²⁶). Thus, colour discrimination in the long-wavelength region relies on the combined activation of L and M cones, whereas short-wavelength discrimination depends on S cones, as L and M cones are weakly responsive and covary significantly in that region.

Addressing spatial visual function in individuals with anomalous trichromacy, Doron et al.²⁷ reported an intriguing advantage for colour-deficient individuals in detecting objects camouflaged in grayscale figures. This enhanced ability to perceive objects in visually challenging environments may contribute to the relatively high prevalence of colour-vision polymorphisms in humans²⁸ focused on image correction techniques specifically designed for observers with colour vision deficiencies. Unlike previous approaches that primarily adjust insensitive colours, this study emphasizes the importance of saliency in the visual attention of colour-deficient observers. The reduced set of relevant colours linked to CVDs in our study highlights the disparities in saliency areas between colour-normal and colour-deficient individuals, emphasizing the need for tailored image correction methods that consider salient regions.

In the work by Tirandaz et al.¹², we already demonstrated that quantization based on relevant colours was an efficient process. However, that study only involved observers with normal colour vision. What are the implications of a similar task now being performed by observers with a colour vision deficiency? On one hand, the process of selecting relevant colours in the image is an encoding process by the encoder (i.e., an observer) that limits the amount of information or resources required to encode a signal (the rate or the number of selected colours, just as it did with observers with normal colour vision). On the other hand, the decoding process by the observer not only involves the loss of fidelity introduced during reconstruction but is also further affected by the fact that the observer is colour defective, and this means that the decoding (i.e., distortion) will be impacted in an additional way. Twomey et al.²⁹ and Gibson et al.³⁰ also confirmed extensive variation in the demand to speak about different regions of colours, with the regions of greatest demand correlating with the colours of salient objects. Thus, colour terms tend to reflect how often speakers need to refer to different colours, and similar to how different colours require different needs from speakers, our work has proven that different paintings (i.e., complex spatio-chromatic sets of colours) demand different communicative needs from individuals with colour vision deficiency. By applying information-theoretic models, Zaslavsky and colleagues^{31,32} have shown that languages adapt their colour categories to maximize communicative success within their perceptual limits emphasizing how communicative need—shaped by the cultural and environmental contexts of speakers—plays a crucial role in shaping colour naming systems. Remarkably, our complexity and accuracy values, as shown in Fig. 9, fall approximately within the same range reported by Zaslavsky et al.²⁵ This alignment suggests that our results are consistent with the theoretical landscape of complexity-accuracy trade-offs. However, it is important to note that the paradigm used by Zaslavsky et al. (optimal colour languages) is fundamentally different from ours (relevant colours), highlighting the novelty of our approach. These are examples about a unified account of how biological, cultural, and cognitive factors influence the way humans categorize and name colours. It is plausible to assume that observers with colour vision deficiencies would follow the same communicative success.

Methods

Image datasets

We used a set of colour images (Fig. 1) that contained representational paintings from the Trecento era to the Romantic era. These images portrayed a variety of subjects, such as rural landscapes, indoor scenes, still life, portraits, and historical events. Provided by the Prado Museum³³, the images were encoded in 24-bit RGB format and ranged from 6,520,320 to 9,682,560 pixels per image. On average, each image contained approximately 1.3×10^5 unique colours within the dataset's bit resolution¹².

The physiological-based model of Machado et al.³⁴ was used to simulate colour vision deficiencies. The simulation operator adapted from Machado et al.³⁴, Eq. (24), was applied to each original colour image to emulate the perception of both dichromats and anomalous trichromats. Within this model, colour vision deficiencies can vary from mild to severe depending on the amount of shift found in the peak sensitivity of the photopigments; we have used five different degrees of severity levels corresponding to 4 nm, 8 nm, 12 nm, 16 nm, and 20 nm, although two degrees of severity ($d=8$ and 20 nm) are shown in this work.

Observers

Adult observers with colour vision deficiencies were selected, provided that their visual optics allowed comfortable viewing of a computer screen. The observers were classified according to the results of the anomaloscope (OCULUS HMC-Anomaloskop USA), widely regarded as the most accurate test for categorizing colour vision deficiencies³⁵. The study was approved by the Research Ethics Committee of the University of Granada (2198/CEIH/2021) and all research was performed in accordance with its relevant guidelines; in addition an informed consent was obtained from all participants and/or their legal guardians. The use of corrective glasses by the participants, if they had them and/or used them in their daily lives, was irrelevant for this study. All the participants (29 observers) were offered the opportunity to undergo colour vision tests such as the Ishihara test or the Farnsworth arrangement test (none of which are invasive) to determine their colour vision conditions. A total of 11 deuteranopes, 11 protanopes, 3 deuteranomalous observers and 4 protanomalous observers participated in the experiment (all men, except one deuteranomalous woman).

Procedure

PsychToolbox3 software³⁶ was used to display the images for the experiment. The participants were seated 70 cm away from a self-calibrated Eizo Colour Edge CG277 27-inch monitor. This monitor automatically calibrates itself via a built-in sensor. The size of each image was adjusted to a maximum width of 35 cm and a maximum height of 26.5 cm. Each subject (wearing their glasses, if required) observed a set of colour images displayed on the screen. During the experiment session, the observers' task was simply to freely gaze at the scene and use the mouse to click on a single location to indicate that, in their judgment, exhibited a relevant colour in the painting. However, the definition of a "relevant colour" was left ambiguous, allowing participants to select as many colours as they desired¹¹. The presentation order of the 20 images shown in Fig. 1 was randomized for each observer. All forward computations were performed by averaging 25 pixels around each selected pixel. Each scene was displayed for a maximum duration of 60 s, but if the participant completed their selection task before that time, they could press a key to proceed to the next image. The subsequent scene appeared after a 1.5 s interval. If the participants became fatigued, they were allowed to pause the session at any time and to resume later. The spatial locations selected by the observer for each image, along with the RGB digital values of those locations, were automatically stored.

Data analysis

The statistical descriptors employed encompassed the colour distribution of the CIEL*a*b* colour components of the obtained relevant colours. Additionally, the colour volume was computed, which represented the palette of available colours within one image and the coverage of the overlap between the distribution of relevant colours (for each observer and painting) and the original gamut of colours.

Distortion, communicative needs, and complexity relationships

An upper limit on the rate of information transmission for any channel, defined by its entropy, was established as a fundamental principle by the information theory, setting a physical boundary on transmission rates for systems such as the brain^{37–39}. Extending this concept to human performance offers a framework for understanding the representation of sensory input, perception, and behaviour. For single-dimensional variations, the estimated channel capacity averages about 2.5 bits, while multidimensional object identification appears unrestricted by simple channel capacity^{37,38}. Mutual information quantifies shared information between variables, indicating their dependence³⁹. In visual processing, a high mutual information suggests strong relationships, helping the visual system identify patterns and objects⁴⁰. Rate-distortion theory explores the balance between compression efficiency and reconstruction quality^{23,41}, underpinning efficient data compression algorithms. Together, mutual information and rate-distortion optimize visual processing: mutual information supports scene representation, and rate-distortion balances compression with quality^{40,42}. Our study focuses on colour image compression and thus examines trade-offs between compression rate and image quality, particularly for colour vision deficiencies.

Estimating mutual information

For a randomly selected pixel from an image, its RGB values $a = (R, G, B)$ can be treated as a single observation of a trivariate discrete random variable A . This variable is characterized by its probability mass function p . The entropy $H(A)$ of A quantifies the uncertainty associated with A and is defined as⁴³

$$H(A) = - \sum_a p(a) \log_2 p(a) \quad (3)$$

where a spans the gamut of possible pixel values. The entropy is expressed in bits when the logarithm is computed using base 2. Thus, for two images represented by random variables A_1 and A_2 with respective probability mass functions p_1 and p_2 , the mutual information $I(A_1; A_2)$ measures the shared information between A_1 and A_2 ⁴³. It is defined as

$$I(A_1; A_2) = H(A_1) + H(A_2) - H(A_1; A_2) \quad (4)$$

where $H(A_1; A_2)$ denotes the joint entropy of A_1 and A_2 . A straightforward way to estimate p involves dividing the colour space into a finite number of bins and counting the frequency of occurrences within each bin. However, this naive approach often introduces bias, particularly when the sample size is limited⁴³. To address this, a bias-corrected entropy estimator proposed by Grassberger can be employed instead³⁸. Using this method,

estimates of the mutual information $I(A_O; A_{RC})$ were obtained, where A_O represents the original RGB image and A_{RC} corresponds to its quantized representation using relevant colours.

Data availability

The images of the paintings analysed in this study are available at <https://www.museodelprado.es/en/the-collection/>. The software for estimating mutual information is available at <https://github.com/imarinfr/klo>. The software for designing and implementing the experiment is available at <http://psychtoolbox.org/>.

Received: 5 December 2024; Accepted: 27 February 2025

Published online: 31 March 2025

References

- Carrasco, M. Visual attention: The past 25 years. *Vis. Res.* **51**, 1484–1525 (2011).
- Li, Z. *Understanding Vision: Theory, Models, and Data* (Oxford University Press, 2014).
- Linhares, J. M., Pinto, P. D. & Nascimento, S. M. The number of discernible colors in natural scenes. *J. Opt. Soc. Am. A* **25**, 2918–2924 (2008).
- Perales, E., Martínez-Verdú, F. M., Linhares, J. M. M. & Nascimento, S. M. C. Number of discernible colors for color-deficient observers estimated from the MacAdam limits. *J. Opt. Soc. Am. A* **27**, 2106–2114 (2010).
- Nascimento, S., Linhares, J., Pastilha, R., Santos, J. & de Almeida, V. Perceived chromatic diversity in dichromacy benefits from the color distributions of natural scenes. *J. Vis.* **16**, 638 (2016).
- Marques, D. N., Gomes, A. E., Linhares, J. M. & Nascimento, S. M. Discrimination of natural colors in anomalous trichromacy and the effects of EnChroma and Vino filters. *Opt. Express* **31**, 18075–18087 (2023).
- Hiramatsu, C. et al. Influence of colour vision on attention to, and impression of, complex aesthetic images. *Proc. Biol. Sci.* **290**, 20231332 (2023).
- Marín-Franch, I. & Foster, D. H. Number of perceptually distinct surface colors in natural scenes. *J. Vis.* **10**(9), 9 (2010).
- Nieves, J. L. & Romero, J. Heuristic analysis influence of saliency in the color diversity of natural images. *Color Res. Appl.* **43**, 713–725 (2018).
- Nieves, J. L., Gomez-Robledo, L., Chen, Y. & Romero, J. Computing the relevant colors that describe the color palette of paintings. *Appl. Opt.* **59**, 1732–1740 (2020).
- Nieves, J. L., Ojeda, J., Gómez-Robledo, L. & Romero, J. Psychophysical determination of the relevant colours that describe the colour palette of paintings. *J. Imaging* **7**, 72 (2021).
- Tirandaz, Z., Foster, D. H., Romero, J. & Nieves, J. L. Efficient quantization of painting images by relevant colors. *Sci. Rep.* **13**, 3034 (2023).
- Linhares, J. M. M. & Nascimento, S. M. C. A chromatic diversity index based on complex scenes. *J. Opt. Soc. Am. A* **29**, A174–A181 (2012).
- Valero, E. M. et al. Is it really possible to compensate for colour blindness with a filter?. *Color. Technol.* **137**, 64–67 (2021).
- Huertas, R., Angel Martínez-Domingo, M., Valero, E. M., Gomez-Robledo, L. & Hernández-Andrés, J. Metasurface-based contact lenses for color vision deficiency: comment. *Opt. Lett.* **45**, 5117–5118 (2020).
- Martínez-Domingo, M. Á., Valero, E. M., Gomez-Robledo, L., Huertas, R. & Hernandez-Andres, J. Spectral filter selection for increasing chromatic diversity in CVD subjects. *Sensors* **20**, 2023 (2020).
- Linhares, J. M., Pinto, P. D. & Nascimento, S. M. The number of discernible colors perceived by dichromats in natural scenes and the effects of colored lenses. *Vis. Neurosci.* **25**, 493–499 (2008).
- Moreira, H., Lillo, J. & Álvaro, L. “Red-Green” or “Brown-Green” Dichromats? The accuracy of dichromat basic color terms metacognition supports denomination change. *Front. Psychol.* **12**, 624792 (2021).
- Lillo, J., Mor eira, H., Álvaro, L. & Davies, I. Basic color term use by red-green dichromats: 1. General description. *Color Res. Appl.* **39**, 360–371 (2013).
- Álvaro, L., Moreira, H., Lillo, J. & Franklin, A. Color preference in red–green dichromats. *Proc. Natl. Acad. Sci.* **112**, 9316–9321 (2015).
- Foster, D. H. & Nascimento, S. M. Little information loss with red-green color deficient vision in natural environments. *iScience* **26**, 107421 (2023).
- Montagner, C., Linhares, J. M. M., Vilarigues, M. & Nascimento, S. M. C. Statistics of colors in paintings and natural scenes. *J. Opt. Soc. Am. A* **33**, 170–177 (2016).
- Morgera, S. D. & Soleymanl, M. R. *Machine Intelligence and Pattern Recognition* 257–275 (Elsevier, 1988).
- Sims, C. R. Rate-distortion theory and human perception. *Cognition* **152**, 181–198 (2016).
- Zaslavsky, N., Kemp, C., Regier, T. & Tishby, N. Efficient compression in color naming and its evolution. *Proc. Natl. Acad. Sci. USA* **115**, 7937–7942 (2018).
- Zhaoping, L., Geisler, W. S. & May, K. A. Human wavelength discrimination of monochromatic light explained by optimal wavelength decoding of light of unknown intensity. *PLoS One* **6**, e19248 (2011).
- Doron, R. et al. Spatial visual function in anomalous trichromats: Is less more?. *PLoS One* **14**, e0209662 (2019).
- Li, J., Feng, X. & Fan, H. Saliency-based image correction for colorblind patients. *Comput. Vis. Med.* **6**, 169–189 (2020).
- Twomey, C. R., Roberts, G., Brainard, D. H. & Plotkin, J. B. What we talk about when we talk about colors. *Proc. Natl. Acad. Sci.* **118**, e2109237118 (2021).
- Gibson, E. et al. Color naming across languages reflects color use. *Proc. Natl. Acad. Sci.* **114**, 10785–10790 (2017).
- Zaslavsky, N., Kemp, C., Tishby, N. & Regier, T. Color naming reflects both perceptual structure and communicative need. *Top. Cognit. Sci.* **11**, 207–219 (2019).
- Zaslavsky, N., Kemp, C., Tishby, N. & Regier, T. Communicative need in colour naming. *Cognit. Neuropsychol.* **37**, 235–240 (2020).
- Masterpieces, Prado Museum, Spain. <https://www.museodelprado.es/en/the-collection> (2022).
- Machado, G. M., Oliveira, M. M. & Fernandes, L. A. A physiologically-based model for simulation of color vision deficiency. *IEEE Trans. Visual. Comput. Graphics* **15**, 1291–1298 (2009).
- Barbur, J. L. & Rodríguez-Carmona, M. Ranking the severity of colour vision loss in congenital deficiency. *Invest. Ophthalmol. Vis. Sci.* **53**, 4137 (2012).
- Kleiner, M., Brainard, D. & Pelli, D. What’s new in Psychtoolbox-3? (2007).
- Marín-Franch, I. & Foster, D. H. Estimating information from image colors: An application to digital cameras and natural scenes. *IEEE Trans. Pattern Anal. Mach. Intell.* **35**, 78–91 (2013).
- Grassberger, P. Entropy Estimates from Insufficient Samplings. Preprint at <https://arxiv.org/abs/physics/0307138> (2008)
- Shannon, C. E. A mathematical theory of communication. *Bell Syst. Tech. J.* **27**, 379–423 (1948).
- Miller, G. A. The magical number seven, plus or minus two: Some limits on our capacity for processing information. *Psychol. Rev.* **63**, 81 (1956).
- Bates, C. J. & Jacobs, R. A. Efficient data compression in perception and perceptual memory. *Psychol. Rev.* **127**, 891 (2020).

42. Warren, W. H. Information is where you find it: Perception as an ecologically well-posed problem. *i-Perception* **12**, 20416695211000370 (2021).
43. Thomas, M. & Joy, A. T. *Elements of Information Theory* (Wiley, 2006).

Acknowledgements

Grant PID2022-139056NB-I00 funded by MICIU/AEI/10.13039/501100011033 by the “European Union”.

Author contributions

J.L.N. and J.R.M. conceived the experiment; J.L.N., J.H.A. and L.G.R. conducted the experiment; and J.L.N. and J.R.M. analysed the results. All the authors reviewed the manuscript.

Funding

Ministerio de Universidades, PID2022-139056NB-I00.

Declarations

Competing interests

The authors declare no competing interests.

Additional information

Correspondence and requests for materials should be addressed to J.L.N.

Reprints and permissions information is available at www.nature.com/reprints.

Publisher’s note Springer Nature remains neutral with regard to jurisdictional claims in published maps and institutional affiliations.

Open Access This article is licensed under a Creative Commons Attribution-NonCommercial-NoDerivatives 4.0 International License, which permits any non-commercial use, sharing, distribution and reproduction in any medium or format, as long as you give appropriate credit to the original author(s) and the source, provide a link to the Creative Commons licence, and indicate if you modified the licensed material. You do not have permission under this licence to share adapted material derived from this article or parts of it. The images or other third party material in this article are included in the article’s Creative Commons licence, unless indicated otherwise in a credit line to the material. If material is not included in the article’s Creative Commons licence and your intended use is not permitted by statutory regulation or exceeds the permitted use, you will need to obtain permission directly from the copyright holder. To view a copy of this licence, visit <http://creativecommons.org/licenses/by-nc-nd/4.0/>.

© The Author(s) 2025